Association of a murine leukaemia stem cell gene signature based on nucleostemin promoter activity with prognosis of acute myeloid leukaemia in patients

Mohamed A.E. Ali [a], Kazuhito Naka [b], Akiyo Yoshida [c], Kyoko Fuse [a], Atsuo Kasada [a], Takayuki Hoshii [a], Yuko Tadokoro [a], Masaya Ueno [a], Kumiko Ohta [a], Masahiko Kobayashi [a], Chiaki Takahashi [c], Atsushi Hirao [a],*

[a] Division of Molecular Genetics, Cancer Research Institute, Kanazawa University, Kakuma-machi, Kanazawa, Ishikawa 920-1192, Japan
[b] Exploratory Project on Cancer Stem Cells, Cancer Research Institute, Kanazawa University, Kakuma-machi, Kanazawa, Ishikawa 920-1192, Japan
[c] Division of Oncology and Molecular Biology, Cancer Research Institute, Kanazawa University, Kakuma-machi, Kanazawa, Ishikawa 920-1192, Japan

ARTICLE INFO

ABSTRACT

Acute myeloid leukaemia (AML) is a heterogeneous neoplastic disorder in which a subset of cells function as leukaemia-initiating cells (LICs). In this study, we prospectively evaluated the leukaemia-initiating capacity of AML cells fractionated according to the expression of a nucleolar GTP binding protein, nucleostemin (NS). To monitor NS expression in living AML cells, we generated a mouse AML model in which green fluorescent protein (GFP) is expressed under the control of a region of the NS promoter (NS–GFP). In AML cells, NS–GFP levels were correlated with endogenous NS mRNA. AML cells with the highest expression of NS–GFP were very immature blast-like cells, efficiently formed leukaemia colonies in vitro, and exhibited the highest leukaemia-initiating capacity in vivo. Gene expression profiling analysis revealed that cell cycle regulators and nucleotide metabolism-related genes were highly enriched in a gene set associated with leukaemia-initiating capacity that we termed the 'leukaemia stem cell gene signature'. This gene signature stratified human AML patients into distinct clusters that reflected prognosis, demonstrating that the mouse leukaemia stem cell gene signature is significantly associated with the malignant properties of human AML. Further analyses of gene regulation in leukaemia stem cells could provide novel insights into diagnostic and therapeutic approaches to AML.

© 2014 Elsevier Inc. All rights reserved.

1. Introduction

Acute myeloid leukaemia (AML) is a heterogeneous neoplastic disorder characterized by substantial cellular heterogeneity. Only a rare subset of cells is assumed to have the ability to self-renew and to initiate and sustain the disease [1]. Understanding the functional regulatory machinery of these leukaemia initiating cells (LICs) is critically important for designing an efficient therapeutic approach, but these cells have not yet been characterized in detail.

Nucleostemin (NS, also known as GNL3) encodes a GTP-binding protein that is mainly located in rRNA-free sites of the nucleolus [2]. NS contributes to ribosomal biogenesis by interacting with nucleolar proteins involved in pre-rRNA processing [3]. Moreover, NS is essential for the maintenance of nucleolar architecture and the integrity of nucleolar RNA–protein complexes [4]. NS also

interacts with telomeric repeat-binding factor 1 (TRF1) to facilitate its degradation, which enhances the maintenance of telomere length [5]. NS and GNL3L form a complex with the telomerase catalytic subunit, human telomerase reverse transcriptase (hTERT) [6]. NS was originally discovered during research on genes that are highly expressed in neural stem cells, embryonic stem (ES) cells, and developing organs during embryogenesis [7]. NS functions as a reprogramming factor for induced pluripotent stem (iPS) cells [8], indicating that NS is essential for the maintenance of the undifferentiated status of ES/iPS cells. In neural stem cells, NS contributes to genomic stability [9], and NS deficiency in neural stem cells causes replication-dependent DNA damage that is associated with defective self-renewal. In haematopoietic stem cells, NS knockdown impairs the long-term reconstitution capacity and induces apoptosis as a result of accumulated DNA damage [10].

We previously generated transgenic mice in which green florescent protein (GFP) is expressed under the control of a particular region of the NS promoter (NS–GFP). In this system,

we successfully identified the stem cell population among neonatal testicular cells, liver cells, and foetal brain tissues [11–13] as well as tumour-initiating cells, conceptually termed 'cancer stem cells,' in brain tumours and germ cell tumours [13,14]. Consistent with our studies, NS-enriched mammary tumour cells are highly tumourigenic [15]. Although the mechanisms are still unclear, there are particular programs that control NS expression and functions that are also commonly involved in maintaining stem cell properties in normal and malignant tissues. Recently, a study with newly diagnosed AML patients reported that high expression of NS is closely correlated with the percentage of immature blast cells and with haematopoietic stem/progenitor cell surface markers and that high NS transcript levels are found in AML patients with poor prognosis [16]; this suggests that NS expression may be an indicator of immature properties of AML cells. In this study, we prospectively evaluated the leukaemia-initiating capacity of subpopulations of AML cells with varying NS expression by using NS-GFP transgenic mice. We found that a leukaemia stem cell gene signature containing genes differentially expressed in cells with high and low NS promoter activity could also be used to stratify human AML patients into distinct clusters that reflected prognosis.

2. Materials and methods

2.1. Generation of an AML model

NS-GFP transgenic mice were generated as described previously [11]. All procedures were performed in accordance with the animal care guidelines of Kanazawa University, Kanazawa, Japan. A murine AML model was generated as previously reported [17]. Briefly, c-Kit$^+$Sca-1$^+$Lineage$^-$ cells isolated from bone marrow (BM) of NS–GFP transgenic mice were infected with a retrovirus carrying *Hoxa9* and *Meis1a* (MSCV-Hoxa9-IRES-Meis1a) and transplanted into lethally irradiated syngeneic mice along with 5×10^5 normal BM mononuclear cells (rescue cells).

2.2. Leukaemia initiating capacity in vitro and in vivo

The leukaemia-initiating capacity of fractionated NS–GFP cells was evaluated with a colony formation assay (MethoCult GF M3434, Stem Cell Technologies Inc., Vancouver, Canada) and with transplantation into lethally irradiated recipient mice, as previously described [18].

2.3. Cell cycle analysis

The recipient mice were sacrificed 2 h after intraperitoneal injection of 5-bromo-2′-deoxyuridine (BrdU, 100 mg/kg, Sigma–Aldrich., Missouri, USA). The fractionated cells were stained with FITC-conjugated anti-BrdU antibody (BD Biosciences, New Jersey, USA) and propidium iodide (PI, 20 μg/ml, Sigma–Aldrich).

2.4. Quantitative RT-PCR analysis

RNA samples were purified from fractionated leukaemia cells (1.5×10^4) using an RNeasy kit (QIAGEN, Tokyo, Japan) and reverse-transcribed using an Advantage RT-for-PCR kit (Clontech, Takara Bio Inc., Shiga, Japan). PCR for NS was performed using a Dice PCR Thermal Cycler (Takara Bio Inc.) as previously reported [11].

2.5. Preprocessing of microarray data

Gene expression profiling of mouse AML cells was performed as described in the Supplementary Methods. Briefly, total RNA was isolated from (a) c-Kit$^-$NS–GFP^{low}, (b) c-Kit$^-$NS–GFP^{middle}, (c) c-Kit$^+$NS-GFP^{middle}, and (d) c-Kit$^+$NS-GFP^{high} cells, followed by cDNA synthesis. cDNA microarray analysis was performed with a GeneChip Mouse 430 2.0 (Affymetrix Inc., High Wycombe, UK). The complete microarray data set is available at the Gene Expression Omnibus (www.ncbi.nlm.nih.gov/geo/, accession number GSE 58032). Unsupervised hierarchical clustering was performed on the normalized and log-transformed data of 17,419 probes. Similarity was measured by Euclidean distance metric, and the average linkage was used to define the linking distance between clusters. To select probes whose expression changed progressively among the 4 subpopulations, we extracted 3494 probes that showed gradual increases or decreases in expression as AML differentiation increased. Among the 3494 probes, 500 probes that exhibited in the largest ratios between c-Kit$^-$NS–GFP^{low} and c-Kit$^+$NS–GFP^{high} were extracted. The 500 probes corresponded to 382 mouse gene symbols, forming the 'leukaemia stem cell gene signature' shown in Supplementary Table 1. Pathway analysis using the 382 mouse gene symbols was performed by using DAVID v6.7 (http://david.abcc.ncifcrf.gov/) with Gene Ontology (GO) and Kyoto Encyclopedia of Genes and Genomes (KEGG). The 382 mouse gene symbols corresponded to 338 human gene symbols, as identified at Mouse Genome Informatics (http://www.informatics.jax.org/).

2.6. Analysis of human AML patient data

We used data from 179 AML patient samples developed by The Cancer Genome Atlas Research Network [19] (http://cancergenome.nih.gov/). For patients clustering, we used 318 human genes from AML patients that are included in the database and were among the 338 human genes in the leukaemia stem cell gene signature. Clustering of AML patients was performed by using the R 'cluster' package, PAM (Partitioning Around Medoids; http://stat.ethz.ch/R-manual/R-patched/library/cluster/html/pam.html).

2.7. Statistical analyses

For analysis of mouse AML samples, statistical differences among multiple groups were evaluated by a one-way ANOVA and Tukey as a post hoc test. Statistical differences in Kaplan–Meier survival curves were determined using the log-rank test. For analysis of human AML data, age of patients, initial white blood cell (WBC) number of peripheral blood, and percent of blasts among mononuclear BM cells were compared among the clusters with Student's *t*-test or a one-way ANOVA/Tukey. Patients' sex, French-American-British (FAB) classification, and molecular risk classification were compared with Fisher's exact test and Bonferroni as a post hoc test. Overall survival was plotted using the Kaplan–Meier estimator and compared with the log-rank test. The statistical analyses were performed using R software, and a two-sided significance level of $\alpha < 0.05$ was used.

3. Results

3.1. Fractionation of living AML cells based on NS expression level

We first investigated whether our NS-GFP reporter system could be used to monitor NS mRNA in AML cells *in vivo*. To do so, we infected c-Kit$^+$Sca-1$^+$Lineage$^-$ BM mononuclear cells from NS-GFP transgenic mice with a retrovirus expressing both the *Hoxa9* and *Meis1a* genes. This procedure generates a well-characterized AML once the transduced cells are transplanted into lethally irradiated syngeneic hosts [20]. As expected, all recipients of NS–GFP transgenic cells transduced with *Hoxa9* and *Meis1a* developed leukaemia. Morphological analysis showed that the
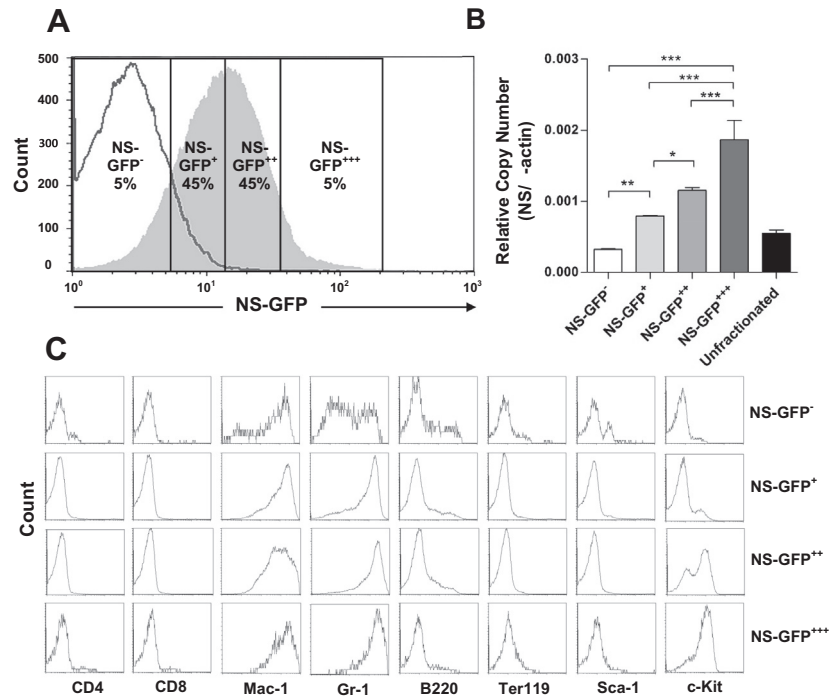
Fig. 1. Characterization of fractionated AML cells by expression levels of NS-GFP. (A) GFP intensity of leukaemia cells derived from NS–GFP transgenic mice. BM cells of recipient mice with AML were analysed by flow cytometry and divided into 4 subfractions according to GFP fluorescence intensity. (B) NS mRNA expression levels. Data are presented as the mean ± SD of the ratios of NS to β-actin mRNA copy numbers in fractionated cells ($n = 3$). *$p < 0.05$; **$p < 0.01$; ***$p < 0.001$, (C) Expression of surface markers, including CD4, CD8, Mac-1, Gr-1, B220, Ter119, Sca-1 and c-Kit on fractionated cells.
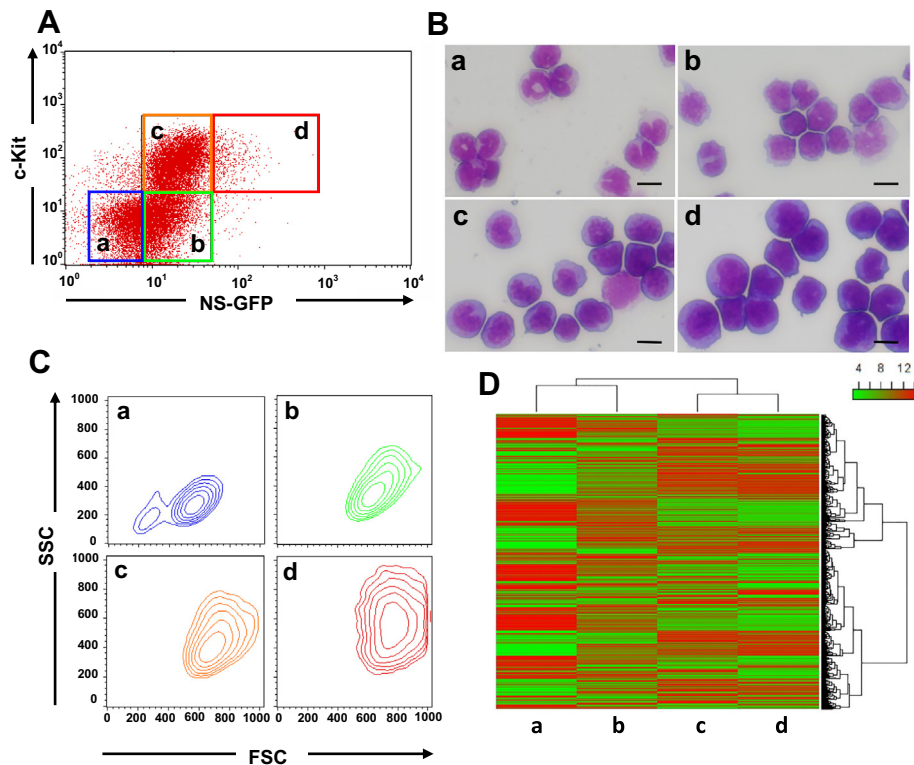
Fig. 2. Enrichment of immature blastic leukaemia cells in the NS-high cell population. (A) Representative data of NS-GFP and c-Kit expression on BM cells in leukaemic mice. AML cells were fractionated into 4 subpopulations: (a) c-Kit⁻NS–GFP^low, (b) c-Kit⁻NS–GFP^middle, (c) c-Kit⁺NS–GFP^middle, (d) c-Kit⁺NS–GFP^high. (B) Morphology of fractionated leukaemia cells. The fractionated AML cells were stained with May-Grünwald–Giemsa staining. (C) Representative data from forward-scattered (FSC) and side-scattered (SSC) light showing cell size of fractionated AML cells. (D) The gene expression profiling of fractionated AML cells. Unsupervised hierarchical clustering was performed on the normalized and log-transformed data of 17,419 probes, similarity was measured by Euclidean distance metric, and the average linkage was used to define the linking distance between clusters. Red and green reflect high and low expression levels, respectively, as indicated in the scale bar.

recipient BM was filled with leukaemia cells, including many blast-like cells and some more mature myeloid-like cells such as neutrophils and monocytes (data not shown), which is categorized as AML with maturation under the WHO classification (FAB Classification M2) [20]. We fractionated the approximately 95% of BM cells that were positive for NS–GFP into 3 subpopulations depending on GFP fluorescence intensity: NS–GFP^{+++} (approximately top 5%), NS–GFP^{++} (next 45%), and NS–GFP^{+} (next lower 45%); the remaining 5% were NS–GFP^{-} (Fig. 1A). GFP fluorescence intensity in all 4 fractions closely paralleled the endogenous NS mRNA expression as measured by RT-PCR (Fig. 1B).

3.2. Correlation of maturation stages of leukaemia cells with NS–GFP level

To characterize the fractionated AML cells, we analysed several surface markers for haematopoietic differentiation (Fig. 1C). As expected, all 4 fractions expressed the myeloid lineage marker Mac-1 but not markers for the T, B, or erythroid lineages. Sca-1, which is expressed in haematopoietic stem cells but not myeloid progenitor cells, was not expressed in any of the fractionated cells. Most NS–GFP^{+++} leukaemia cells expressed c-Kit, consistent with the positive correlation between NS and c-KIT [16]. The expression of c-Kit decreased with decreasing GFP intensity, so that the NS–GFP^{++} and NS–GFP^{+} cell populations consisted of both c-Kit^{+} and c-Kit^{-} cells (Fig. 2A), and NS–GFP^{-} cells did not express c-Kit. Therefore, we designated these populations as (a) c-Kit^{-}NS–GFP^{low}, (b) c-Kit^{-}NS–GFP^{middle}, (c) c-Kit^{+}NS–GFP^{middle}, and (d) c-Kit^{+}NS–

GFP^{high}, reflecting the combined patterns of NS–GFP and c-Kit expression.

The morphology of leukaemia cells differed remarkably among the subpopulations (Fig. 2B). The c-Kit^{+}NS–GFP^{high} cells appeared to be very immature blast-like cells with large nuclei, whereas c-Kit^{-}NS–GFP^{low} cells appeared to be mature myeloid cells with lobular nuclei. The NS–GFP^{middle} cells (both c-Kit^{+} and c-Kit^{-}) had intermediate morphological features. Consistent with these findings, the c-Kit^{+}NS–GFP^{high} cells were larger than cells in the other subpopulations as evaluated by flow cytometry (Fig. 2C). We next examined the gene expression profiles of each of the 4 leukaemic cell fractions to see if there was a relationship between GFP fluorescence intensity and pattern of gene expression. The gene expression profile of c-Kit^{+}NS–GFP^{high} cells was closer to that of c-Kit^{+}NS–GFP^{middle} cells than to that of c-Kit^{-}NS–GFP^{middle} and c-Kit^{-}NS–GFP^{low} cells, whereas the gene expression profile of c-Kit^{-}NS–GFP^{low} was closest to that of c-Kit^{-}NS–GFP^{middle} (Fig. 2D). These progressive changes in morphology, cell surface marker profile, and gene expression profile suggested that c-Kit^{+}NS–GFP^{high} leukaemia cells differentiate into c-Kit^{+}NS–GFP^{middle} and c-Kit^{-}NS–GFP^{middle} cells, which subsequently differentiate into c-Kit^{-}NS–GFP^{low} cells.

3.3. Characterization of undifferentiated leukaemia cells

We evaluated the cell cycle status of the fractionated NS–GFP leukaemia cells *in vivo* by measuring BrdU incorporation and DNA content (Fig. 3A). The proportion of BrdU-positive cells was
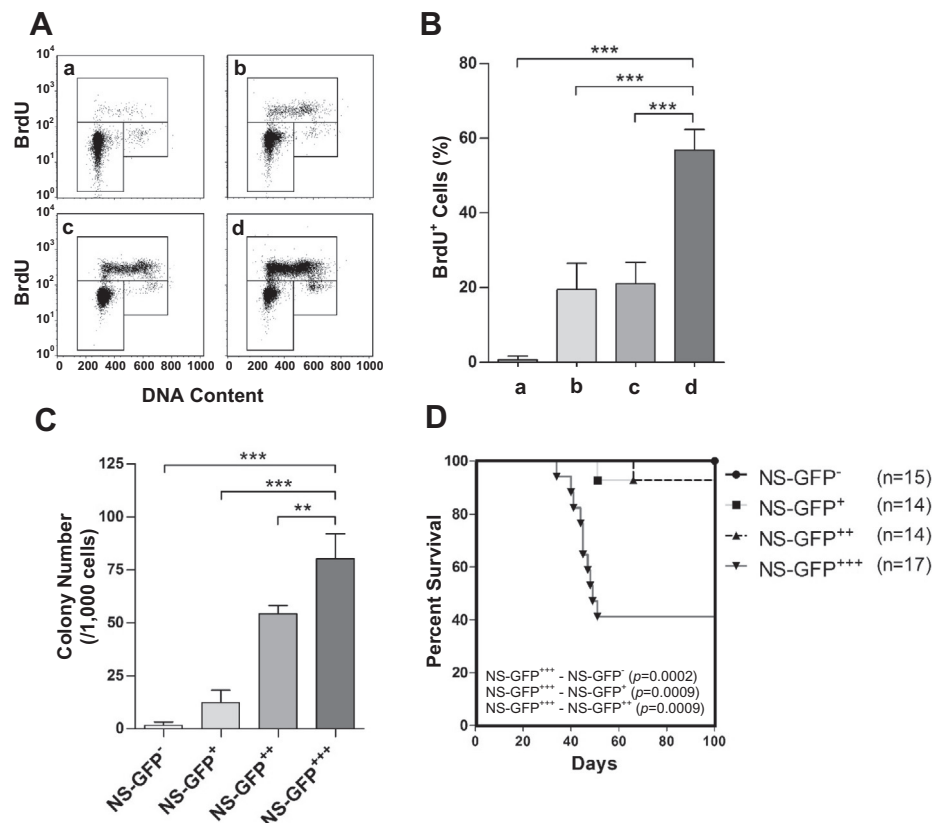
Fig. 3. Correlation of NS expression with leukaemia-initiating capacity. (A and B) Cell cycle analysis with BrdU incorporation and DNA content. The leukaemic mice were sacrificed 2 h after BrdU injection, followed by staining of fractionated AML cells, including (a) c-Kit^{-}NS–GFP^{low}, (b) c-Kit^{-}NS–GFP^{middle}, (c) c-Kit^{+}NS–GFP^{middle}, and (d) c-Kit^{+}NS–GFP^{high} with an anti-BrdU antibody and PI. (A) Representative data are shown. (B) The data are presented as the mean ± SD of the percentage of BrdU^{+} cells among all cells in the fraction ($n = 3$). ***$p < 0.001$ (C) Colony-forming capacity of fractionated leukaemia cells. The fractionated AML cells shown in Fig. 1A were cultured in methylcellulose media. The data shown are the mean ± SD of the number of colonies ($n = 3$). **$p < 0.01$; ***$p < 0.001$, (D) Survival of recipient mice with fractionated AML cells. Ten leukaemia cells from each fraction shown in Fig. 1A were transplanted along with 5×10^5 bone marrow competitor cells (rescue cells) into lethally irradiated mice. Significant differences between NS–GFP^{+++} and other fractionated AML cells were observed.

significantly higher in c-Kit⁺NS–GFPʰⁱᵍʰ cells more than the other subpopulations (Fig. 3B), indicating that these immature blast-like cells were actively cycling. To characterise the gene signature of undifferentiated leukaemia cells, we selected 3494 probes whose expression gradually increased or decreased along with the progressive changes among the 4 subpopulations. Among these 3494 probes, we further selected 500 probes (382 genes) that exhibited the largest ratios between differentiated (c-Kit⁻NS–GFPˡᵒʷ) and undifferentiated (c-Kit⁺NS–GFPʰⁱᵍʰ) cells (Supplementary Table 1). Consistent with the data shown in Fig. 1B, the NS gene was included in the gene set. Pathway analysis with the 382 genes showed that cell cycle regulators and nucleotide metabolism-related genes were highly enriched (Supplementary Table 2). These data are consistent with the dramatic differences in cell cycle status between the cell fractions (Fig. 3B).

### 3.4. Enrichment of LICs in cells expressing high levels of NS–GFP in vitro and in vivo

To investigate properties of the fractionated cells, we performed in vitro colony-forming assays with the 4 subpopulations of AML cells shown in Fig. 1A (NS–GFP⁺⁺⁺, NS–GFP⁺⁺, NS–GFP⁺, and NS–GFP⁻). We found that NS–GFP⁺⁺⁺ cells exhibited the highest colony-forming ability among the subpopulations. Both NS–GFP⁺⁺⁺ and NS–GFP⁺⁺ leukaemia cells readily formed colonies, whereas NS-GFP⁻ did not (Fig. 3C), indicating that NS expression is correlated with colony-forming ability.

Next, we evaluated leukaemia-initiating capacity in vivo with a transplantation assay. When we transplanted 100 cells of each of the 4 fractionated leukaemia cell subpopulations into lethally irradiated mice, all recipient mice developed leukaemia (data not

shown), indicating that the frequency of LICs was very high. Therefore, to distinguish between the cell subpopulations, we transplanted 10 cells of each. In this condition, we found that only the NS–GFP⁺⁺⁺ cells generated a secondary leukaemia (Fig. 3D). Thus, LICs are enriched in cells with highest level of NS–GFP.

3.5. Association of a murine leukaemia stem cell gene signature with prognosis of human AML patients

Finally, we investigated whether NS is associated with the properties of human AML cells. To do so, we first evaluated NS gene expression in human AML patients by using the public database developed by the Cancer Genome Atlas (TCGA) Research Network [19]. Unexpectedly, we did not find a correlation between human NS expression and FAB classification, molecular risk, or prognosis (Supplementary Fig. 1). We therefore evaluated the relationship between the leukaemia stem cell gene signature shown above and characteristics of AML patients. We selected 318 human genes corresponding to the 500 mouse probes described above (Supplementary Table 1). Using this human gene set, we performed a clustering algorithm related to the k-medoids algorithm (Partitioning Around Medoids; PAM) for 179 AML patient samples. Because the clustering analysis showed that the average silhouette width was higher for $k = 2$ or 3 than for $k = 4$ or 5, we first stratified AML patients into two clusters (Cluster 1, $n = 34$; Cluster 2, $n = 145$) (Fig. 4A). Patients in the two clusters showed significant differences in age, number of WBCs, FAB classification, and molecular risks (Supplementary Table 3A). Cluster 1 consisted of younger patients who had lower WBC numbers than patients in Cluster 2. All patients with M3 FAB classification were included in Cluster 1, whereas all patients whose leukaemia was classified as M0,
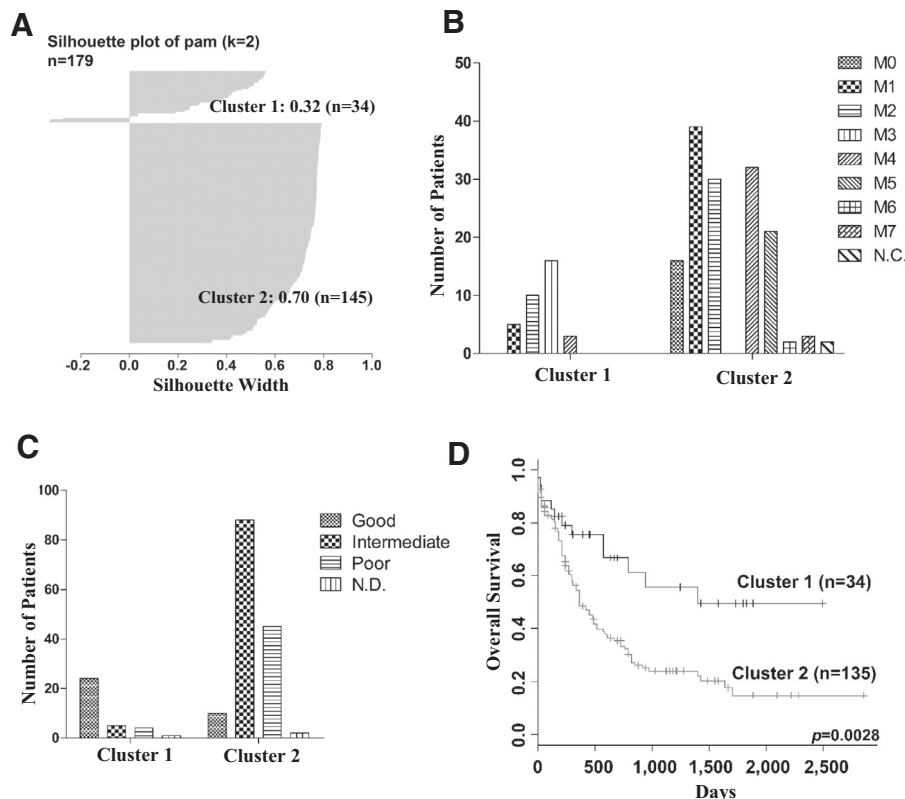
Fig. 4. Correlation of prognosis of AML patients with the leukaemia stem cell gene signature. (A) Clustering of 179 AML patients by a clustering algorithm (PAM) using the leukaemia stem cell gene signature (318 human genes). Clustering data ($k = 2$) with silhouette width are shown. Average silhouette width is 0.63. (B and C) Numbers of patients with FAB classification (B) or molecular risk classification (C) are shown. (N.C.) not classified. (N.D.) no data. (D) Overall survival of the clustered AML patients. Cluster 1 patients had a significantly higher survival rate than Cluster 2 patients.

M6, or M7, which are relatively poor prognostic types, were included in Cluster 2 (Fig. 4B). Molecular risk classification showed that patients in Cluster 1 exhibited more good prognostic factors and fewer intermediate and poor prognostic factors than those in Cluster 2 (Fig. 4C and Supplementary Table 3A). Consistent with these findings, the overall survival rate was significantly higher for Cluster 1 patients than for Cluster 2 patients (Fig. 4D). When we stratified AML patients into three clusters, we found that one cluster mainly consisted of patients whose leukaemia was classified as M3 and that there were significant differences in prognosis between the clusters (Supplementary Fig. 2 and Table 3B). Thus, the gene signature of leukaemia stem cells in a mouse model is correlated with the malignant status of human AML.

4. Discussion

We successfully identified LICs by monitoring NS expression in a mouse AML model. In this system, endogenous NS correlated well with the undifferentiated status of leukaemia cells *in vivo*. In normal haematopoiesis, NS is more highly expressed in myeloid progenitors and haematopoietic stem cells than in differentiated haematopoietic cells [10]. Because a recent study indicated that AML stem cells are immunophenotypically similar to progenitors, including lymphoid-primed multipotent progenitors and granulocyte–macrophage progenitors [21], the higher expression of NS in myeloid progenitor cells may be conserved in leukaemia stem cells. Our data in the AML mouse model suggest that NS plays a critical role in maintaining undifferentiated status in AML cells, as has been shown in ES/iPS cells [8].

There are critical differences in the characteristics of AML between mouse and human. We found that NS gene expression itself was not correlated with the prognostic characteristics of AML in patients in the TCGA database, which was inconsistent with a previously reported result [16]. Although mouse NS was included in the leukaemia stem cell gene signature, NS expression levels were not significantly different among AML patient clusters in our study (data not shown), presumably due to heterogeneity among patients in the regulation of human NS expression. In addition, LICs from patient samples and the experimental mice also exhibited critical differences. For example, although human LICs are rare and cycle slowly [22], c-Kit$^+$NS–GFP^{high} leukaemia cells were actively cycling in our mouse model. Therefore, the gene signature identified in this experiment may not be directly associated with the endogenous pattern of NS expression. Even though NS itself may not function as a potent driver of malignant status in AML patients, our data suggest that a network of genes associated with NS promoter activity affects the malignant status of human and mouse AML cells.

In clinical investigations, high NS expression is associated with poor prognosis in breast cancer [23], oesophageal cancer [24], and gastric and liver cancer [25]. Therefore, the core network of the leukaemia stem cell gene signature may be conserved in stem cells in solid tumours. In this study, we identified a gene set associated with AML that included cell cycle and nucleotide metabolism-related genes. These genes may coordinate stem cell properties with response to DNA damage and telomere stability to control self-renewal activity in normal and malignant cells, including solid tumours. Further analysis of NS-related genes may contribute to the understanding of the factors that regulate a variety of cancers.

Conflict of interest

The authors declare no conflict of interest.

Acknowledgments

Appendix A. Supplementary data

Supplementary data associated with this article can be found, in the online version, at http://dx.doi.org/10.1016/j.bbrc.2014.06.066.

References

[1] S.J. Horton, B.J. Huntly, Recent advances in acute myeloid leukemia stem cell biology, Haematologica 97 (2012) 966–974.
[2] J.C. Politz, I. Polena, I. Trask, D.P. Bazett-Jones, T. Pederson, A nonribosomal landscape in the nucleolus revealed by the stem cell protein nucleostemin, Mol. Biol. Cell 16 (2005) 3401–3410.
[3] L. Romanova, A. Grand, L.Y. Zhang, S. Rayner, N. Katoku-Kikyo, S. Kellner, N. Kikyo, Critical role of nucleostemin in pre-rRNA processing, J. Biol. Chem. 284 (2009) 4968–4977.
[4] L. Romanova, S. Kellner, N. Katoku-Kikyo, N. Kikyo, Novel role of nucleostemin in the maintenance of nucleolar architecture and integrity of small nucleolar ribonucleoproteins and the telomerase complex, J. Biol. Chem. 284 (2009) 26685–26694.
[5] L.J. Meng, J.K. Hsu, Q.B. Zhu, T. Lin, R.Y.L. Tsai, Nucleostemin inhibits TRF1 dimerization and shortens its dynamic association with the telomere, J. Cell Sci. 124 (2011) 3706–3714.
[6] N. Okamoto, M. Yasukawa, C. Nguyen, V. Kasim, Y. Maida, R. Possemato, T. Shibata, K.L. Ligon, K. Fukami, W.C. Hahn, K. Masutomi, Maintenance of tumor initiating cells of defined genetic composition by nucleostemin, Proc. Natl. Acad. Sci. U.S.A. 108 (2011) 20388–20393.
[7] R.Y.L. Tsai, R.D.G. McKay, A nucleolar mechanism controlling cell proliferation in stem cells and cancer cells, Gene Dev. 16 (2002) 2991–3003.
[8] J. Qu, J.M. Bishop, Nucleostemin maintains self-renewal of embryonic stem cells and promotes reprogramming of somatic cells to pluripotency, J. Cell Biol. 197 (2012) 731–745.
[9] L. Meng, T. Lin, G. Peng, J.K. Hsu, S. Lee, S.Y. Lin, R.Y. Tsai, Nucleostemin deletion reveals an essential mechanism that maintains the genomic stability of stem and progenitor cells, Proc. Natl. Acad. Sci. U.S.A. 110 (2013) 11415–11420.
[10] M. Yamashita, E. Nitta, G. Nagamatsu, Y.M. Ikushima, K. Hosokawa, F. Arai, T. Suda, Nucleostemin is indispensable for the maintenance and genetic stability of hematopoietic stem cells, Biochem. Biophys. Res. Commun. 441 (2013) 196–201.
[11] M. Ohmura, K. Naka, T. Hoshii, T. Muraguchi, H. Shugo, A. Tamase, N. Uema, T. Ooshio, F. Arai, K. Takubo, G. Nagamatsu, I. Hamaguchi, M. Takagi, M. Ishihara, K. Sakurada, H. Miyaji, T. Suda, A. Hirao, Identification of stem cells during prepubertal spermatogenesis via monitoring of nucleostemin promoter activity, Stem Cells 26 (2008) 3237–3246.
[12] H. Shugo, T. Ooshio, M. Naito, K. Naka, T. Hoshii, Y. Tadokoro, T. Muraguchi, A. Tamase, N. Uema, T. Yamashita, Y. Nakamoto, T. Suda, S. Kaneko, A. Hirao, Nucleostemin in injury-induced liver regeneration, Stem Cells Dev. 21 (2012) 3044–3054.
[13] A. Tamase, T. Muraguchi, K. Naka, S. Tanaka, M. Kinoshita, T. Hoshii, M. Ohmura, H. Shugo, T. Ooshio, M. Nakada, K. Sawamoto, M. Onodera, K. Matsumoto, M. Oshima, M. Asano, H. Saya, H. Okano, T. Suda, J. Hamada, A. Hirao, Identification of tumor-initiating cells in a highly aggressive brain tumor using promoter activity of nucleostemin, Proc. Natl. Acad. Sci. U.S.A. 106 (2009) 17163–17168.
[14] N. Uema, T. Ooshio, K. Harada, M. Naito, K. Naka, T. Hoshii, Y. Tadokoro, K. Ohta, M.A. Ali, M. Katano, T. Soga, Y. Nakanuma, A. Okuda, A. Hirao, Abundant nucleostemin expression supports the undifferentiated properties of germ cell tumors, Am. J. Pathol. 183 (2013) 592–603.
[15] T. Lin, L. Meng, Y. Li, R.Y. Tsai, Tumor-initiating function of nucleostemin-enriched mammary tumor cells, Cancer Res. 70 (2010) 9444–9452.
[16] Y. You, X.Q. Li, J.N. Zheng, Y.H. Wu, Y.L. He, W. Du, P. Zou, M. Zhang, Transcript level of nucleostemin in newly diagnosed acute myeloid leukemia patients, Leuk. Res. 37 (2013) 1636–1641.
[17] J. Lessard, G. Sauvageau, Bmi-1 determines the proliferative capacity of normal and leukaemic stem cells, Nature 423 (2003) 255–260.
[18] T. Hoshii, Y. Tadokoro, K. Naka, T. Ooshio, T. Muraguchi, N. Sugiyama, T. Soga, K. Araki, K. Yamamura, A. Hirao, MTORC1 is essential for leukemia propagation but not stem cell self-renewal, J. Clin. Invest. 122 (2012) 2114–2129.
[19] Cancer Genome Atlas Research, Genomic and epigenomic landscapes of adult de novo acute myeloid leukemia, N. Engl. J. Med. 368 (2013) 2059–2074.
[20] E. Kroon, J. Krosl, U. Thorsteinsdottir, S. Baban, A.M. Buchberg, G. Sauvageau, Hoxa9 transforms primary bone marrow cells through specific collaboration with Meis1a but not Pbx1b, EMBO J. 17 (1998) 3714–3725.
[21] N. Goardon, E. Marchi, A. Atzberger, L. Quek, A. Schuh, S. Soneji, P. Woll, A. Mead, K.A. Alford, R. Rout, S. Chaudhury, A. Gilkes, S. Knapper, K. Beldjord, S.

Begum, S. Rose, N. Geddes, M. Griffiths, G. Standen, A. Sternberg, J. Cavenagh, H. Hunter, D. Bowen, S. Killick, L. Robinson, A. Price, E. Macintyre, P. Virgo, A. Burnett, C. Craddock, T. Enver, S.E. Jacobsen, C. Porcher, P. Vyas, Coexistence of LMPP-like and GMP-like leukemia stem cells in acute myeloid leukemia, Cancer Cell 19 (2011) 138–152.

[22] F. Ishikawa, S. Yoshida, Y. Saito, A. Hijikata, H. Kitamura, S. Tanaka, R. Nakamura, T. Tanaka, H. Tomiyama, N. Saito, M. Fukata, T. Miyamoto, B. Lyons, K. Ohshima, N. Uchida, S. Taniguchi, O. Ohara, K. Akashi, M. Harada, L.D. Shultz, Chemotherapy-resistant human AML stem cells home to and engraft within the bone-marrow endosteal region, Nat. Biotechnol. 25 (2007) 1315–1321.

[23] T. Kobayashi, K. Masutomi, K. Tamura, T. Moriya, T. Yamasaki, Y. Fujiwara, S. Takahashi, J. Yamamoto, H. Tsuda, Nucleostemin expression in invasive breast cancer, BMC Cancer 14 (2014) 215.

[24] G. Zhang, Q. Zhang, Q. Zhang, L. Yin, S. Li, K. Cheng, Y. Zhang, H. Xu, W. Wu, Expression of nucleostemin, epidermal growth factor and epidermal growth factor receptor in human esophageal squamous cell carcinoma tissues, J. Cancer Res. Clin. Oncol. 136 (2010) 587–594.

[25] S.J. Liu, Z.W. Cai, Y.J. Liu, M.Y. Dong, L.Q. Sun, G.F. Hu, Y.Y. Wei, W.D. Lao, Role of nucleostemin in growth regulation of gastric cancer, liver cancer and other malignancies, World J. Gastroenterol. 10 (2004) 1246–1249.